ADVANCES IN ATMOSPHERIC SCIENCES, VOL. 28, NO. 2, 2011, 464–476

Projection of Future Precipitation Change over China with a High-Resolution Global Atmospheric Model

FENG Lei[1,2] (冯 蕾), ZHOU Tianjun*[1] (周天军), WU Bo[1] (吴 波), Tim LI[3], and Jing-Jia LUO[4]

[1]*State Key Laboratory of Numerical Modeling for Atmospheric Sciences and Geophysical Fluid Dynamics, Institute of Atmospheric Physics, Chinese Academy of Sciences, Beijing* 100029

[2]*Graduate University of the Chinese Academy of Sciences, Beijing* 100049

[3]*IPRC and University of Hawaii, Hawaii, USA*

[4]*Research Institute for Global Change, Japan Agency for Marine-Earth Science and Technology, Japan*

(Received 25 January 2010; revised 21 May 2010)

ABSTRACT

Projections of future precipitation change over China are studied based on the output of a global AGCM, ECHAM5, with a high resolution of T319 (equivalent to 40 km). Evaluation of the model's performance in simulating present-day precipitation shows encouraging results. The spatial distributions of both mean and extreme precipitation, especially the locations of main precipitation centers, are reproduced reasonably. The simulated annual cycle of precipitation is close to the observed. The performance of the model over eastern China is generally better than that over western China. A weakness of the model is the overestimation of precipitation over northern and western China. Analyses on the potential change in precipitation projected under the A1B scenario show that both annual mean precipitation intensity and extreme precipitation would increase significantly over southeastern China. The percentage increase in extreme precipitation is larger than that of mean precipitation. Meanwhile, decreases in mean and extreme precipitation are evident over the southern Tibetan Plateau. For precipitation days, extreme precipitation days are projected to increase over all of China. Both consecutive dry days over northern China and consecutive wet days over southern China would decrease.

Key words: future precipitation change, high-resolution AGCM simulation, extreme precipitation

Citation: Feng, L., T. J. Zhou, B. Wu, T. Li, and J.-J. Luo, 2011: Projection of future precipitation change over China with a high-resolution global atmospheric model. *Adv. Atmos. Sci.*, **28**(2), 464–476, doi: 10.1007/s00376-010-0016-1.

1. Introduction

There is increasing observational evidence indicating that extreme precipitation events (both in terms of frequency and intensity) are sensitive to global climate change (Karl et al., 1995; Easterling et al., 2000). Extreme precipitation events over regions where total precipitation is increasing are likely to increase as well. Even over regions where total precipitation is decreasing, or remains unchanged, extreme precipitation events may still increase (IPCC, 2007a). Increasing extreme precipitation events have led to more frequent flood disasters over central East China in recent decades (Yu and Zhou, 2007; Zhai et al., 2008; Zhou et al., 2008a, 2009a). To cope with these disasters, it is essential to understand the underlying reasons for changes in extreme precipitation, and further to project precipitation change under global warming scenarios.

Climate models play a crucial role in simulating and understanding the past, present, and future climate (Zhou et al., 2007). However, the resolutions of current state-of-the-art global climate models are generally coarse. For example, the horizontal resolu-

*Corresponding author: ZHOU Tianjun, zhoutj@lasg.iap.ac.cn

tions of the coupled models which participated in the Fourth Assessment Report for the Intergovernmental Panel on Climate Change (IPCC AR4) are mainly in the range of 125–400 km. Indeed, in the third phase of the Coupled Model Intercomparison Project (CMIP3), an analysis of the models used for IPCC AR4 revealed limitations of the current state-of-the-art coupled climate models in simulating spatial patterns of twentieth-century surface air temperature on the regional scale (Zhou and Yu, 2006), casting a shadow upon their capability in projecting credible geographical distributions of future climate change. Almost all of the IPCC AR4 coupled models tend to overestimate the frequency of light precipitation and underestimate the intensity of extreme precipitation (IPCC, 2007b; Li, 2007). As the spatial scale of precipitation events is often smaller than the grid sizes used by the IPCC AR4 models, model-simulated grid-mean precipitation would likely be lower in intensity than point observations (Wehner et al., 2010).

Models with coarse resolutions might, therefore, underestimate the intensity of precipitation events. Indeed, it has been noted previously that, with increasing model resolution, simulated precipitation intensity tends to be closer to the observed (Li et al., 2010a). In addition, low-resolution climate models may also show bias in reproducing the spatial distribution of days with different levels of precipitation intensity (Zhang and Ding, 2008). To improve the simulation of precipitation, much effort has been devoted to the development of high-resolution models. For example, simulation of the mei-yu (also called as Changma in Korea and Baiu in Japan) rain bands of the East Asian summer monsoon has been improved substantially in terms of geographical distribution by increasing the horizontal resolution (Kusunoki et al., 2006). Increasing the horizontal and vertical resolution can also reduce bias in extreme precipitation simulation, both in terms of intensity and spatial distribution (Tang et al., 2006). By performing a series of sensitivity experiments with different model resolutions, Gao et al. (2006) emphasized that increasing model resolution is important to improve the simulation of monsoon precipitation over East Asia. All of these studies highlight the importance of employing high-resolution climate models in the study of East Asian precipitation.

Given the potential advantages of high-resolution models for better simulation of precipitation over China, in this paper we analyze the output of a high-resolution global climate model: ECHAM5, version T319, which has a horizontal resolution of approximately 40 km. We will systematically evaluate the performance of this high-resolution climate model in reproducing present-day precipitation over China. Based on this, potential changes in extreme precipitation under the IPCC A1B scenario (a "middle of the road" estimate of future greenhouse gas emissions) as projected by the model will be analyzed. To our knowledge, this is the first attempt at examining the performance of such a high-resolution global climate model in the simulation of both mean and extreme precipitation over China.

The paper is organized as follows. The model experiment and observational data are introduced in section 2. The model's ability to simulate present-day precipitation over China is evaluated in section 3. Future precipitation change under the IPCC A1B scenario, including the mean state and extreme precipitation, are discussed in section 4. Finally, a summary of the major findings of this work is presented in section 5.

2. Model description, experimental design, and observational data

2.1 *Model description and experimental design*

The analysis is based on the output of a climate change experiment with a high-resolution version of the ECHAM5 model, developed by the Max Planck Institute for Meteorology (Roechner et al., 2003). The horizontal resolution of this model is T319 [corresponding to a grid size of about 40 km; 960 (lon) $\times$ 480 (lat) grid points], with 31 levels in the vertical direction. To save computation resource, two time-slice integrations were performed to represent the typical present-day and future climates (Bengtsson et al., 2007). These two integrations covered the period 1980–2000 (hereafter, 20th-EXP) and 2080–2100 (hereafter, 21st-EXP), respectively. The atmospheric composition, sea surface temperature, and sea ice cover used to force ECHAM5 were obtained from a set of climate change experiments simulated by an ocean–atmosphere coupled model, ECHAM5/MPI-OM (Jungclaus et al., 2006). The horizontal resolution of the atmospheric component of this coupled model is T63 [192 (lon) $\times$ 96 (lat) grid points]. This low-resolution coupled model simulation was driven by observed historical greenhouse gases and sulphate aerosols from 1860–2000 and greenhouse gas forcing under the IPCC A1B scenario from 2001–2100. This method is an approach used to achieve dynamical downscaling, i.e. adopting higher resolution global atmospheric models to generate finer climate information, but using lower-resolution AOGCM data as their boundary conditions (IPCC, 2007c). For more detailed information about the time-slice experiment, readers are referred to Bengtsson et al. (1996, 2007).

Table 1. Definitions and units of rainfall indices used in this paper. (RR is daily precipitation)

ID	Definitions	Units
R5day	maximum consecutive five-day precipitation	mm
R1day	maximum one-day precipitation	mm
SDII	annual total precipitation divided by the number of wet days (defined as RR$\geqslant$1.0 mm) in the year	mm d^{-1}
Rnn	annual count of days when RR$\geqslant$nn mm (nn is a user defined threshold)	d
CDD	maximum number of consecutive days with RR<1 mm	d
CWD	maximum number of consecutive days with RR$\geqslant$1 mm	d
R95	annual total PRCP when RR>95th percentile	mm
PRCTOT	total PRCP in wet days (RR$\geqslant$1 mm)	mm

In this paper, we analyze the output of two 20-year (1980–1999 and 2080–2099) simulations.

2.2 *Observational precipitation data*

The observational precipitation dataset over East Asia (5°–60°N, 65°–155°E) developed by Xie et al. (2007) was used to evaluate the simulation of present-day precipitation in the 20th-EXP. The data covers the period 1962–2002, and the resolution is 0.5° (lat) × 0.5° (lon). It was constructed by using gauge observations at over 2200 stations collected from several independent sources. The precipitation field has been adjusted by Parameter-Elevation Regressions on Independent Slopes Model (PRISM) monthly precipitation climatology to correct the bias caused by orographic effects.

2.3 *Precipitation indices*

Several precipitation indices based on daily precipitation were used to evaluate the model results and future precipitation change projection (Peterson, 2005). These include mean precipitation (PRCPTOT, SDII) and extreme precipitation (R95, R5day, R1day) indices; level of precipitation intensity (days) indices; and others, including those based on measures of "dryness" (CDD) and "wetness" (CWD). Definitions of these indices are provided in Table 1, and more details can be found at http://cccma.seos.uvic.ca/ETCCDMI/software.shtml.

Data quality control and calculation of the indices were performed by using the Fortran Program FClimDex (also available from the above website). These precipitation indices and the calculation method are widely used in the extreme climate research community (Zhai et al., 2005; Alexander et al., 2006; You et al., 2008).

For the analysis of the annual cycle of precipitation, the PRCPTOT and R1day indices were calculated for each month, and their averages over individual subregions for the whole period are used. For the other analysis, the indices were calculated for each year, and the climatological mean is used. Annual indices were calculated if no more than 15 days of data were missing in a year. For R95, the whole period is used as a base period in this study. The significance of precipitation change projection are examined based on the Student's t-test.

3. Evaluation of the present-day precipitation simulation

3.1 *Annual mean precipitation*

The PRCPTOT and SDII indices (see Table 1) derived from the observation and the model simulation are shown in Figs. 1a–1d. There is no significant difference in the distribution of PRCPTOT (Figs. 1a and 1c) between the observation and simulation. Several observed large precipitation centers are reproduced well by the model, including those over the Sichuan Basin (28°–32°N, 100°–105°E), the middle and lower reaches of the Yangtze River (25°–28°N, 110°–120°E), and the southern part of northeastern China. The topography-induced intense precipitation over the Tibetan Plateau is pronounced in the high-resolution model. Although the simulated precipitation over the southeastern Tibetan Plateau is larger than that derived from the observation, it should be noted that there are not enough observational stations to reflect actual precipitation distribution over the plateau area. The artificial precipitation center on the eastern edge of the Tibetan Plateau (around 31°N, 102°E), which is evident in many coarse-resolution GCM simulations (Yu et al., 2000; Gao et al., 2001, 2004; Zhou and Li, 2002; Chen et al., 2010), is still apparent, but much reduced. From the difference map for PRCPTOT (Fig. 1e) between the simulation and observation, the major biases can be seen over northern and western China. The model overestimates the precipitation over the Tibetan Plateau and northern China by more than 50%, while it underestimates the precipitation in the Tarim and Jungar basins by more than 50%. This underestimation of precipitation over the basins might be attributed to few or no observations being available.

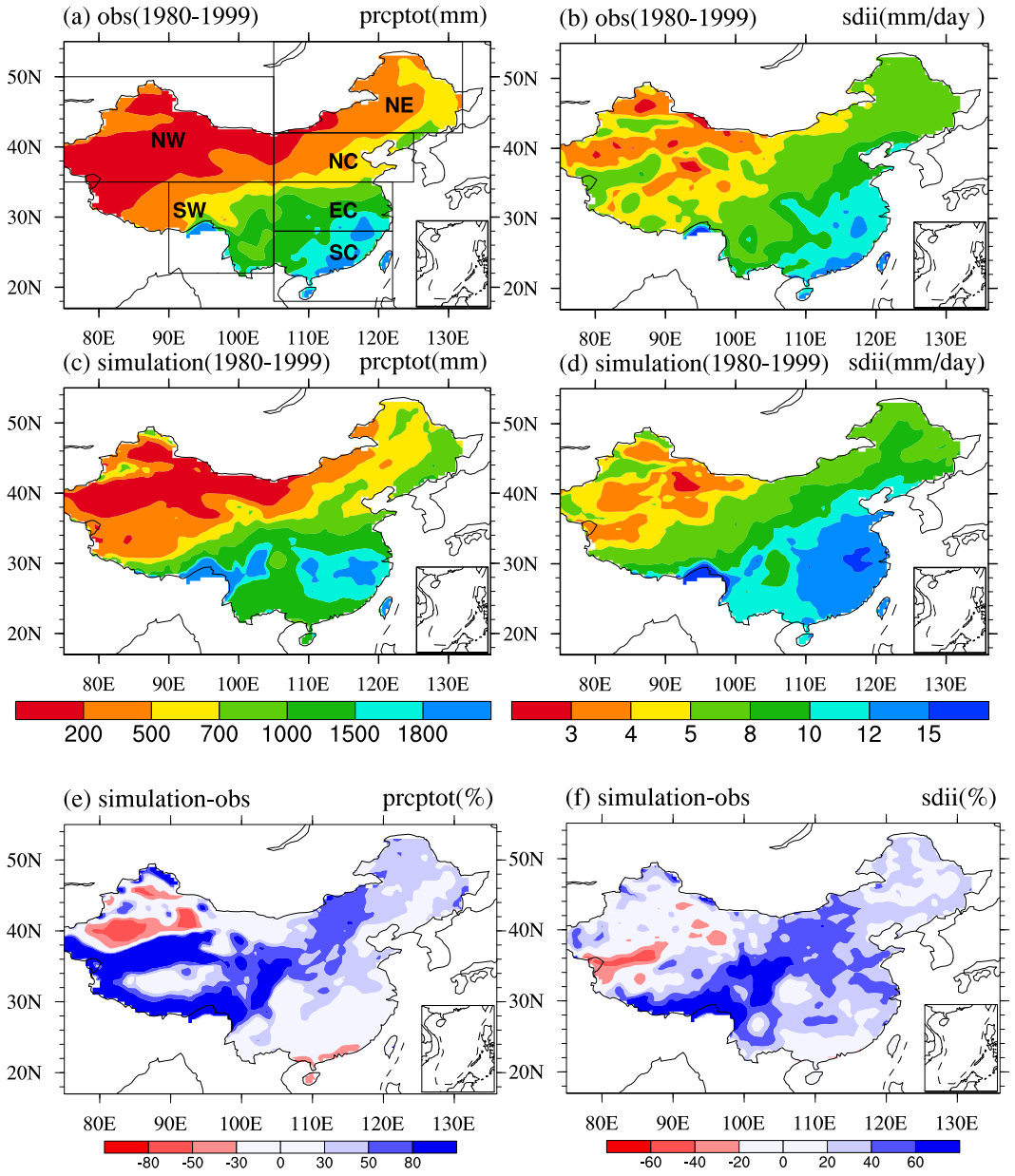

Fig. 1. (a) Observed annual mean total precipitation (PRCPTOT, units: mm) and (b) precipitation intensity (SDII, units: mm d^{-1}) during the period 1980–1999; (c) and (d) are the same as (a) and (b), but for the 20th-EXP. (e) The difference in PRCPTOT between the 20th-EXP and the observation (units: % of observation values). (f) Same as (e) but for SDII. Boxes in (a) illustrate the six sub-regions of China (see section 3.3).

Precipitation there is interpolated from stations surrounding the basin (Gao et al., 2008). For SDII (Figs. 1b and 1d), the model captures well the large precipitation centers over the lower reaches of the Yangtze River. However, the simulated precipitation intensity is much larger than that derived from the observation. The difference for SDII results (Fig. 1f) between the simulation and observation is similar to that for PRCPTOT, except for the magnitude.

3.2 *Extreme precipitation*

The annual mean extreme precipitation indices derived from the observation and simulation are shown in Fig. 2. As can be seen, the model generally reproduces the spatial patterns of R95 (Figs. 2a and 2c) and R5day (Figs. 2b and 2d). Most large centers of R95 are reasonably simulated by the model, such as those in the southeastern Tibetan Plateau, Sichuan Basin, the lower reaches of the Yangtze River, and in

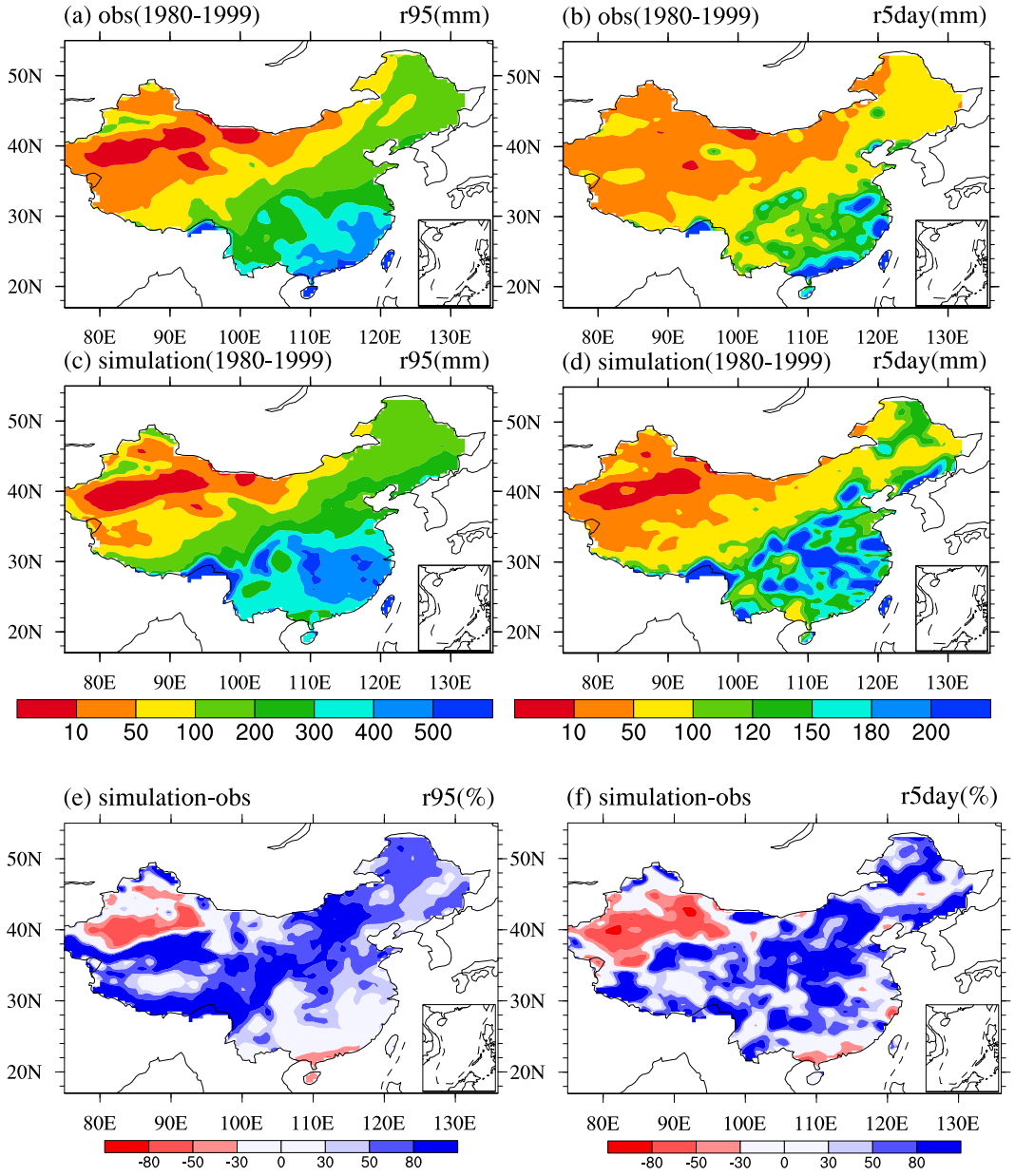

Fig. 2. (a) Observed annual mean of the 95th percentile of precipitation amount (R95, units: mm) and (b) the maximum five-day precipitation (R5day, units: mm) during the period 1980–1999; (c) and (d) are the same as (a) and (b), but for the 20th-EXP. (e) The difference in R95 between the 20th-EXP and the observation (units: % of observation values). (f) Same as (e) but for R5day.

the southern part of northeastern China. However, the large extreme precipitation center over the southern part of South China (18°–23°N, 108°–120°E) is missing in the simulated results. For R5day, the model exhibits more regional signals than the observation. The impact of high-resolution topography on the precipitation is evident. The difference maps for R95 (Fig. 2e) and R5day (Fig. 2f) between the simulation and observation show that the largest bias is located over the areas with complex topography; for example, the Tibetan Plateau and the Tarim Basin. The bias is at least partially caused by insufficient distribution of observational stations (with a prevalence of low level stations), while model deficiency may be another reason. The R5day index over eastern China also shows a large bias and fine-scale features, similar to that over the Tibetan Plateau.

3.3 *Annual cycle of precipitation*

For convenience of discussion, we divide China into six regions (depicted in Fig. 1a): Northwest China (NW: 35°–50°N, 75°–105°E); Southwest China (SW:

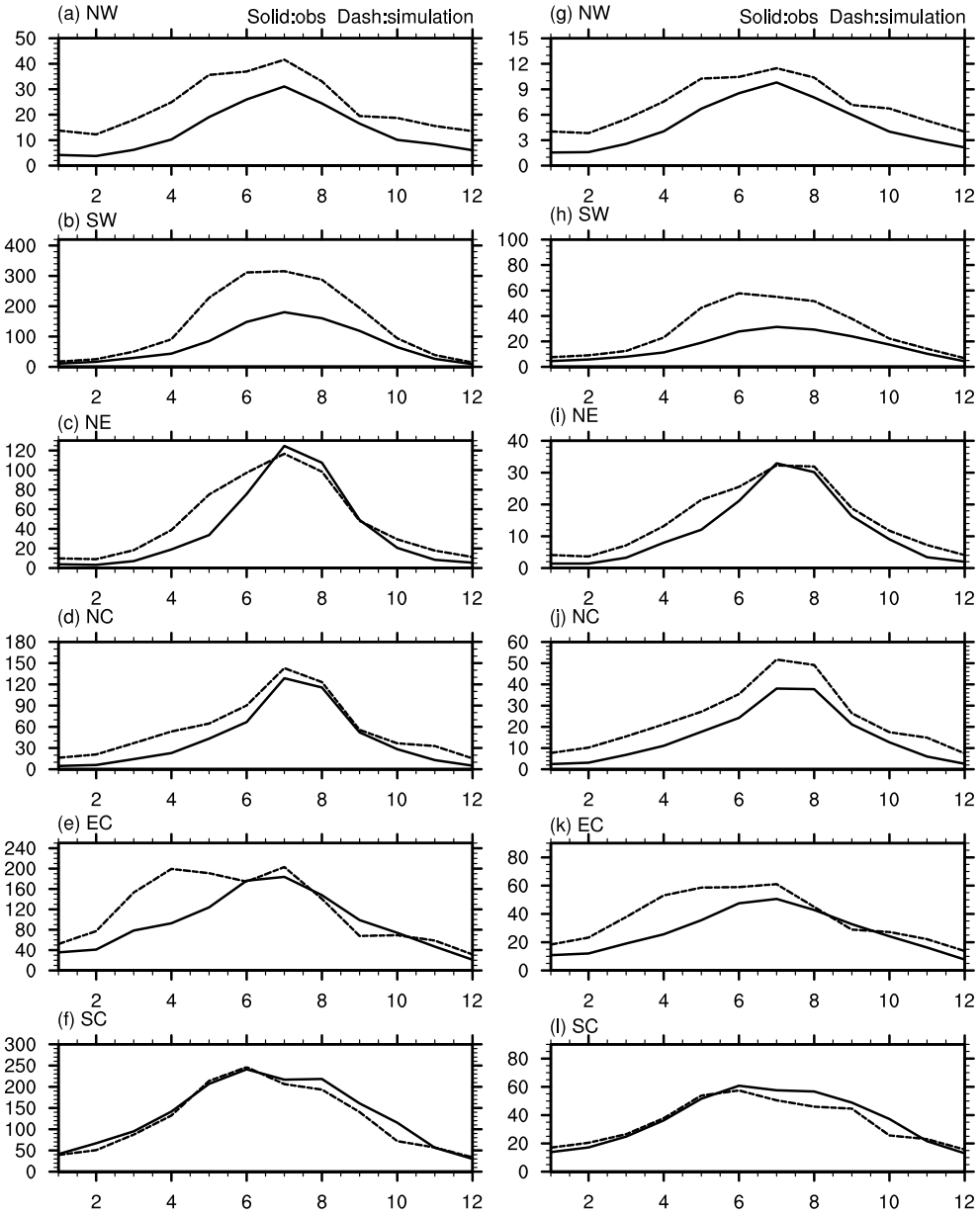

Fig. 3. (a–f) Annual cycle of monthly total precipitation amount (PRCPTOT, units: mm) averaged over six sub-regions: Northwest China (NW), Southwest China (SW), Northeast China (NE), North China (NC), East China (EC), and South China (SC) (boxes shown in Fig. 1a). (g–l) Same as (a–f), but for the monthly maximum one-day precipitation (R1day, units: mm). The abscissa axis is months. The solid and dashed lines represent observed and the 20th-EXP results, respectively.

22°–35°N, 90°–105°E); Northeast China (NE: 42°–55°N, 105°–132°E); North China (NC: 35°–42°N, 105°–125°E); East China (EC: 28°–35 ° N, 105°–122°E); and South China (SC: 18°–28°N, 105°–120°E). From Figs. 3a–3f, it can be seen that the seasonal evolution of monsoon precipitation over China is reproduced realistically by the model. However, the spatially-averaged monthly mean PRCPTOT index is overestimated in most areas, especially in Northwest China (Fig. 3a) and Southwest China (Fig. 3b). In Southwest China, the difference between the simulation and observation is more evident in summer, while in Northwest China, the bias is evident throughout the year. Over Northeast China (Fig. 3c), North China (Fig. 3d), East China (Fig. 3e), and South China (Fig. 3f), the annual cycle of precipitation is captured

well by the high-resolution model, both in amplitude and the month with maximum precipitation. A minor bias appears in spring and autumn, with precipitation being overestimated in Northeast China and North China and underestimated in South China. One exception can be seen over East China, where spring precipitation is overestimated. The simulated monthly mean R1day index (Figs. 3g–3l) resembles well the PRCPTOT index. In regions where total precipitation is overestimated, extreme precipitation is also overestimated.

The above analysis suggests that this high-resolution model can realistically reproduce observed precipitation patterns, including the mean and extreme precipitation events, although some biases are still evident. The rain belt in central eastern China, which always tends to be shifted northward by low-resolution climate models (Zhou and Li, 2002; Gao et al., 2004; Li et al., 2010b; Zhou et al., 2008b; Chen et al., 2010), is simulated well by the high-resolution model. The model can also realistically capture the annual cycle of precipitation over eastern China. Therefore, this model shows reasonably good ability in simulating precipitation over China. Recent studies have indicated that the ECHAM5 model is one of the most advanced climate models for reproducing present climate (Bengtsson et al., 2007), as well as the variability modes of Asian-Australian monsoon precipitation (Zhou et al., 2009b).

The high resolution is possibly an important reason for the improvement in model accuracy. For example, it improves substantially the underestimation of precipitation amounts and regional signals, which are common problems in many low-resolution models (Li et al., 2010a). Giorgi and Marinucci (1996) found that increasing resolution leads to precipitation increases over the Europe in a regional climate model. A similar result was also found for East Asia (Gao et al., 2006). Such improvements may be due to the fact that a higher resolution allows for a better description of complex topography and better reproduction of small-scale atmospheric dynamics (Bell et al., 2004).

The reasonably good performance of the high-resolution model in simulating present-day precipitation provides confidence to use it for projecting future precipitation change. We analyze and discuss the results of this application in the following section.

4. Projected precipitation change

4.1 *Annual mean precipitation*

The percentage changes in annual mean PRCPTOT and SDII in the period 2080–2099 relative to 1980–1999 are shown in Fig. 4. In this figure, regions

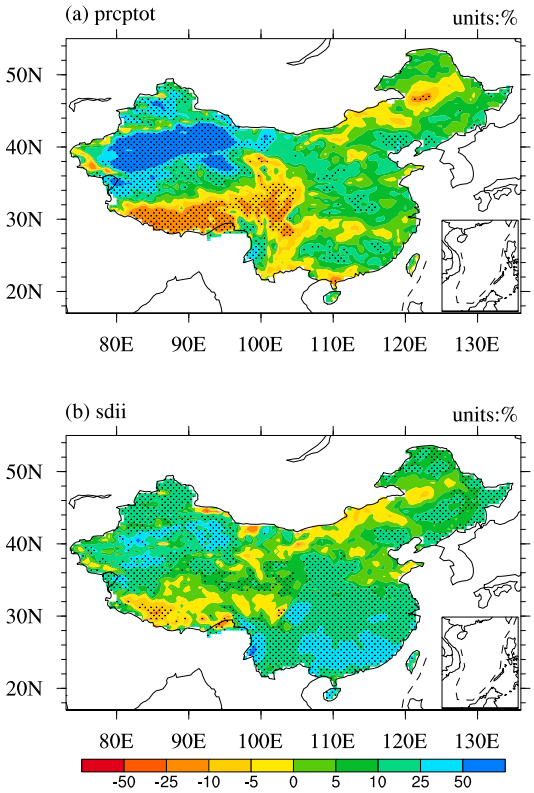

Fig. 4. (a) Percentage change in annual mean total precipitation (PRCPTOT, units: mm) in the 21st-EXP relative to that in the 20th-EXP. (b) The same as (a), but for precipitation intensity (SDII, units: mm d^{-1}). Stippling indicates statistical significance at the 10% level based on the Student's t test (same in Figs. 5, 6 and 7).

where future precipitation changes are statistically significant at the 10% level based on the Student's t-test are highlighted with stippling. The main increase in PRCPTOT is found over northwestern China (Fig. 4a), sometimes increasing by as much as 50%, although the absolute increase is less than 50 mm per year. Some weak increases can be seen over the northern Tibetan Plateau, as well as most parts of southeastern China, northern China, and northeastern China. A decrease is evident over the southern Tibetan Plateau. The projected change pattern in PRCPTOT over western China is close to that derived from a regional climate model, RegCM3, with a horizontal resolution of 20 km (Gao et al., 2008), even though a different A2 scenario and projection period (2070–2100) were applied in their study. This consistency implies that the precipitation change pattern over western China under global warming might be robust. Over eastern China, except in parts of the Yangtze River-Huaihe River area (30°–35°N, 110°–122°E) and northeastern China, the PRCPTOT change exhibits a different trend from that projected by RegCM3. The different response

to global warming reflects the large uncertainty in future precipitation change over the East Asian monsoon area. For SDII change (Fig. 4b), there is a prevailing increase (exceeding 10%) in precipitation intensity over southeastern China. Moreover, SDII increases coherently over northwestern and northeastern China. A decrease is found over the southern Tibetan Plateau and parts of northern China.

4.2 *Extreme precipitation*

The increase in R95 spreads over most parts of China, with the exception of the southern Tibetan Plateau (Fig. 5a). Again, statistically significant regions are highlighted in the figure by stippling. The geographic features of the projected change in R5day are as remarkable as those for R95 (cf. Fig. 5a and Fig. 5b). The scattered and not-well-organized extreme precipitation change centers can be seen over most parts of China. The maximum increasing and decreasing percentages are up to 50% and 25%, respectively. Compared with mean precipitation change, future extreme precipitation increases with greater magnitude and more spatial coherence because of an increase in the moisture content in a warming climate (Allen and Ingram, 2002). In addition, the change in extreme precipitation shows many more features than total precipitation on the regional scale. This is because ECHAM5, being a high-resolution model, can better resolve the mesoscale topography, which tends always to be smoothed by coarse-resolution models. Also, extreme precipitation is greatly influenced by the shape of nearby mountain ranges and the direction of wind flow.

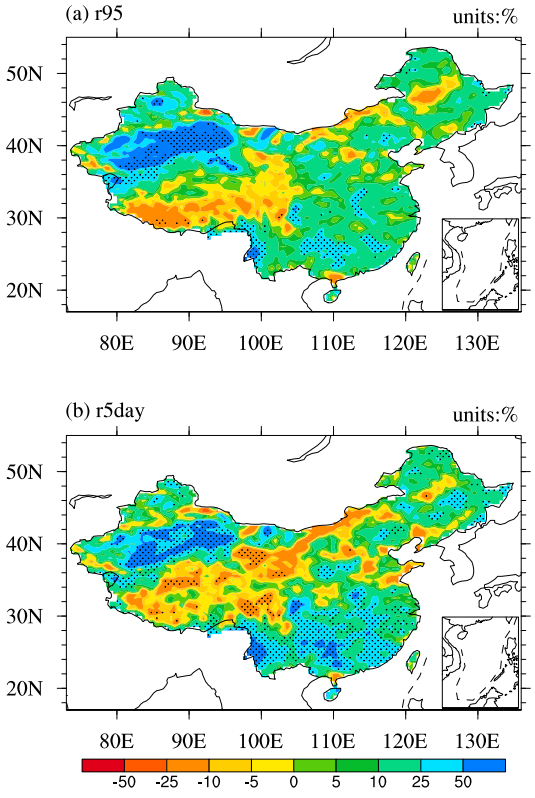

Fig. 5. (a) Percentage change in the 95th percentile of precipitation amount (R95, units: mm) in the 21st-EXP relative to that in the 20th-EXP. (b) The same as (a), but for the maximum five-day precipitation (R5day, units: mm).

4.3 *Precipitation intensity days*

We divide the precipitation intensity into four levels: 0.1–9.9 mm d^{-1} (light precipitation); 10.0–24.9 mm d^{-1} (moderate precipitation); 25.0–49.9 mm d^{-1} (heavy precipitation); and $\geqslant$50.0 mm d^{-1} (torrential precipitation). Projected changes in the number of days featuring precipitation at each of these levels are shown in Fig. 6. Over northwestern China, the change in light precipitation days shows a large increase in the Tarim Basin and a small decrease in northern areas. Moderate and heavy precipitation days increase greatly over the whole of northwestern China. The change in torrential precipitation days is not significant, due to the low precipitation intensity in this region. Over southeastern China, the most significant feature is that the light and moderate precipitation days decrease, while the heavy and torrential precipitation days increase. However, the change in torrential precipitation days does not exceed the 10% level of statistical significance, indicating a large uncertainty. The situation over northeastern China resembles that over southeastern China, except for its central region. The change in precipitation days over northern and central China is not spatially consistent and shows more fine-scale characteristics than that over other areas. Despite some uncertainty in the results over the Tibetan Plateau, the number of days featuring the first three intensity levels would possibly decrease, while the highest level would increase over the southern Plateau. All levels of precipitation days would increase over the northern Plateau.

In summary, the changes in the number of days featuring different levels of precipitation intensity over China under this global warming scenario are as follows. Over southern China and the southern Tibetan Plateau, with high precipitation intensity, lighter precipitation days would decrease and heavier precipitation days would increase. Over northern China and northwestern China, with low precipitation intensity, days of all levels of precipitation would increase. Generally speaking, there would be a decreasing tendency for lighter precipitation days and an increasing ten-

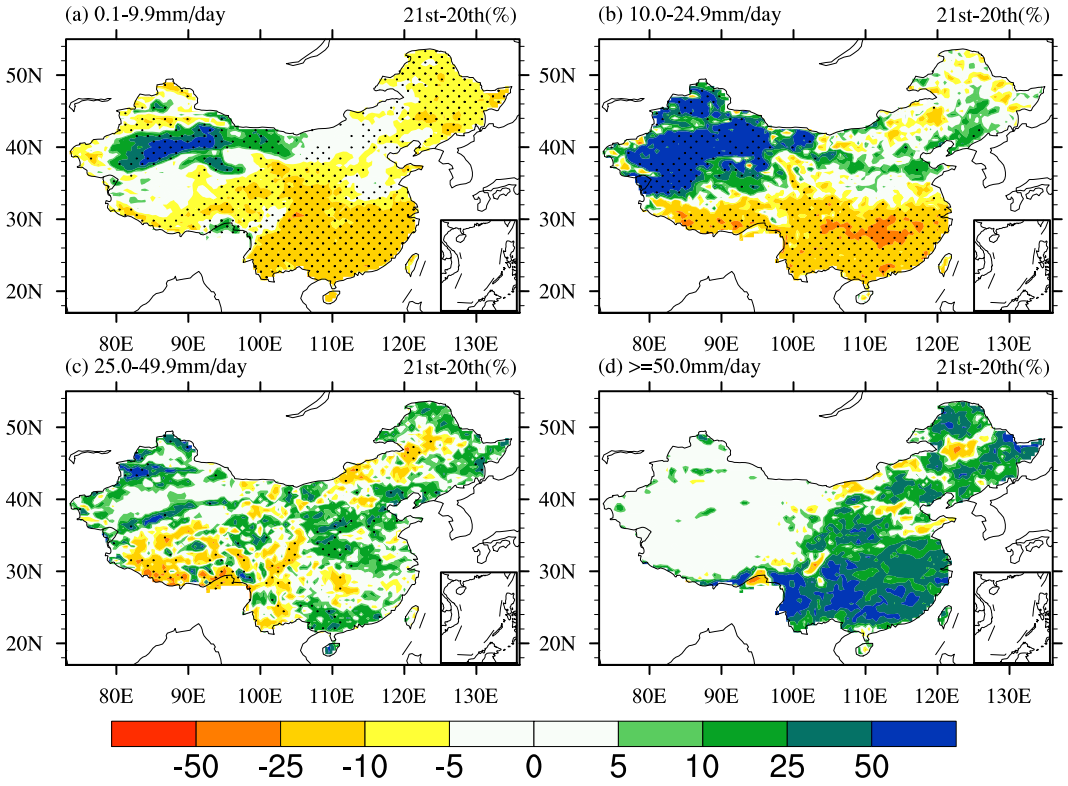

Fig. 6. Percentage change in different levels of precipitation intensity days in the 21st-EXP relative to the 20th-EXP: (a) 0.1–9.9 mm d^{-1}; (b) 10.0–24.9 mm d^{-1}; (c) 25.0–49.9 mm d^{-1}; (d) $\geqslant$50.0 mm d^{-1}.

dency for heavier precipitation days in a warming climate over China. The decrease in lighter precipitation may be attributed to the increasing temperature, which makes it harder for air to reach dew-point temperature (Qian et al., 2007).

4.4 *Consecutive dry and wet days*

To investigate changes in precipitation comprehensively, we also analyze the changes in consecutive dry days (CDD) (Fig. 7a) and consecutive wet days (CWD) (Fig. 7b). Changes in CDD show a north–south difference over China. A significant increase in CDD can be seen over most parts of southern China and small regions of northwestern China. A significant decrease in CDD is apparent in most other areas. CWD tends to decrease significantly over southern China. Over northern China, the number of CWD is small, and hence the change in CWD is limited. Consequently, according to these projected changes in CDD and CWD, most parts of northern China might become wetter in the future, while southern China might become drier.

4.5 *Annual cycle of precipitation*

The future monthly PRCPTOT (Figs. 8a–8f) and R1day (Figs. 8g–8l) show similar seasonal changes. Over Northwest China (Fig. 8a), North China (Fig. 8d), and East China (Fig. 8e), total and extreme precipitation might decrease in summer and increase in the other three seasons in the future. In Southwest China (Fig. 8b) and South China (Fig. 8f), there is an increase in total and extreme precipitation in the summer half of the year (April–September) and a decrease in the winter half of the year (October–March). The monthly total and extreme precipitation over Northeast China (Fig. 8c) would increase in almost all seasons during the period 2080–2099. It should be noted that, over Northeast and East China, although monthly PRCPTOT decreases in summer, monthly R1day still tends to increase.

5. Summary and discussion

5.1 *Summary*

The precipitation change under the IPCC A1B scenario for the period 2080–2099 relative to 1980–1999 has been studied using the output of a 40-km-mesh global AGCM, ECHAM5. As far as the authors are aware, this is the first attempt at examining the performance of a high-resolution global model in projecting future precipitation change over China. The key find-

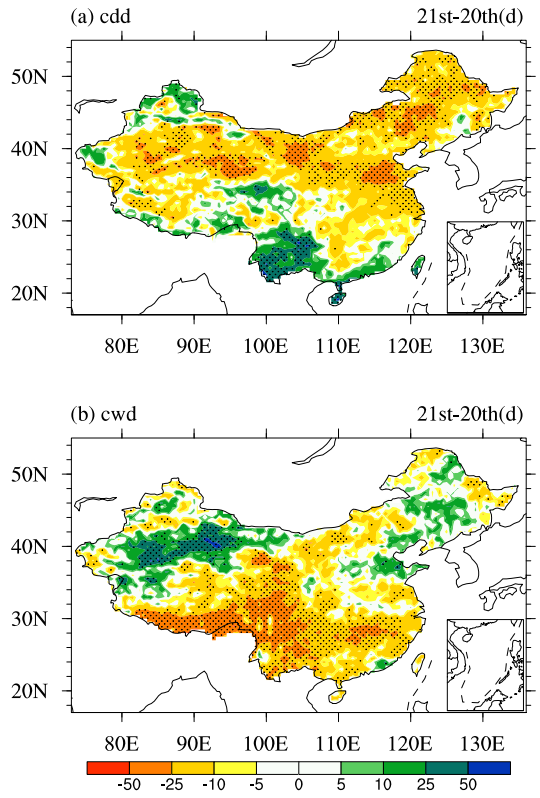

Fig. 7. (a) Absolute change in consecutive dry days (CDD, units: d) in the 21st-EXP relative to the 20th-EXP. (b) The same as (a), but for consecutive wet days (CWD).

ings can be summarized as follows.

(1) Compared with coarse-resolution models, ECHAM5 (T319 version) shows much improvement in simulating the spatial patterns of precipitation, especially the main precipitation centers. The annual cycle of the precipitation over eastern China is reproduced well. Additionally, results from this model provide prominent topography-induced structure and fine-scale geographic features, especially for extreme precipitation. Therefore, using a high-resolution climate model to simulate realistically the precipitation over China is clearly very important.

(2) Under the A1B scenario for the period 2080–2099, ECHAM5 predicts that annual mean total precipitation would increase over most parts of eastern China and the whole of northwestern China. The main decrease is found over the southern Tibetan Plateau and the central part of northeastern China. The annual mean precipitation intensity would likely to increase significantly over southeastern China, by more than 10%.

(3) Projected changes in extreme precipitation also show an increase over most parts of China, except over the southern Tibetan Plateau. ECHAM5 predicts extreme precipitation to increase by more than 25% over most parts of eastern China, higher than the increase in mean precipitation. Meanwhile, the fine-scale features of the potential changes in extreme precipitation are more remarkable, compared with mean precipitation.

(4) Projections by ECHAM5 also show an increase in heavier precipitation days and a decrease in lighter precipitation days over most parts of China, especially in southeastern China. CDD over northern China is projected to decrease by more than 25%, while CDD (CWD) over southern China would likely to increase (decrease), indicating the potential enhanced droughts over southern China, but weakened droughts over northern China.

(5) Potential changes in monthly extreme precipitation averaged over individual sub-regions are consistent with those in total precipitation. The monthly total and extreme precipitation over Northwest China, North China, and East China are projected to decrease in summer and increase in the other three seasons. The situation over Southwest China and South China is exactly the opposite. The predicted tendency in Northeast China for the monthly total and extreme precipitation is to increase throughout almost all of the year, with the percentage increase in the winter half of the year being larger than that in the summer half of the year.

5.2 *Discussion*

Projected precipitation change by the high-resolution ECHAM5 under IPCC A1B scenario is distinguishable from results produced by existing low-resolution global climate models. Seven IPCC AR4 models with a relatively higher level of confidence projected a prevailing increase in precipitation intensity and extreme precipitation over all of China (Jiang et al., 2009). Multi-model ensemble results derived from IPCC AR4 coupled models have also indicated that precipitation would increase over most parts of China (Li and Zhou, 2010). However, large uncertainty has been raised regarding future climate change projection according to the estimates of model spread (Li and Zhou, 2010). Note that the IPCC AR4 models (or formally the CMIP3 models for IPCC AR4) are actually low-resolution models. The present analysis, based on results from a high-resolution model, was conceived in order to enrich our understanding of potential future changes in precipitation over China. Of note, for example, is that the rate of increase in annual precipitation intensity projected by ECHAM5 (more than 2 mm d^{-1}) is larger than that derived from the CMIP3 multi-model ensemble (less than 1 mm d^{-1}) (Li and

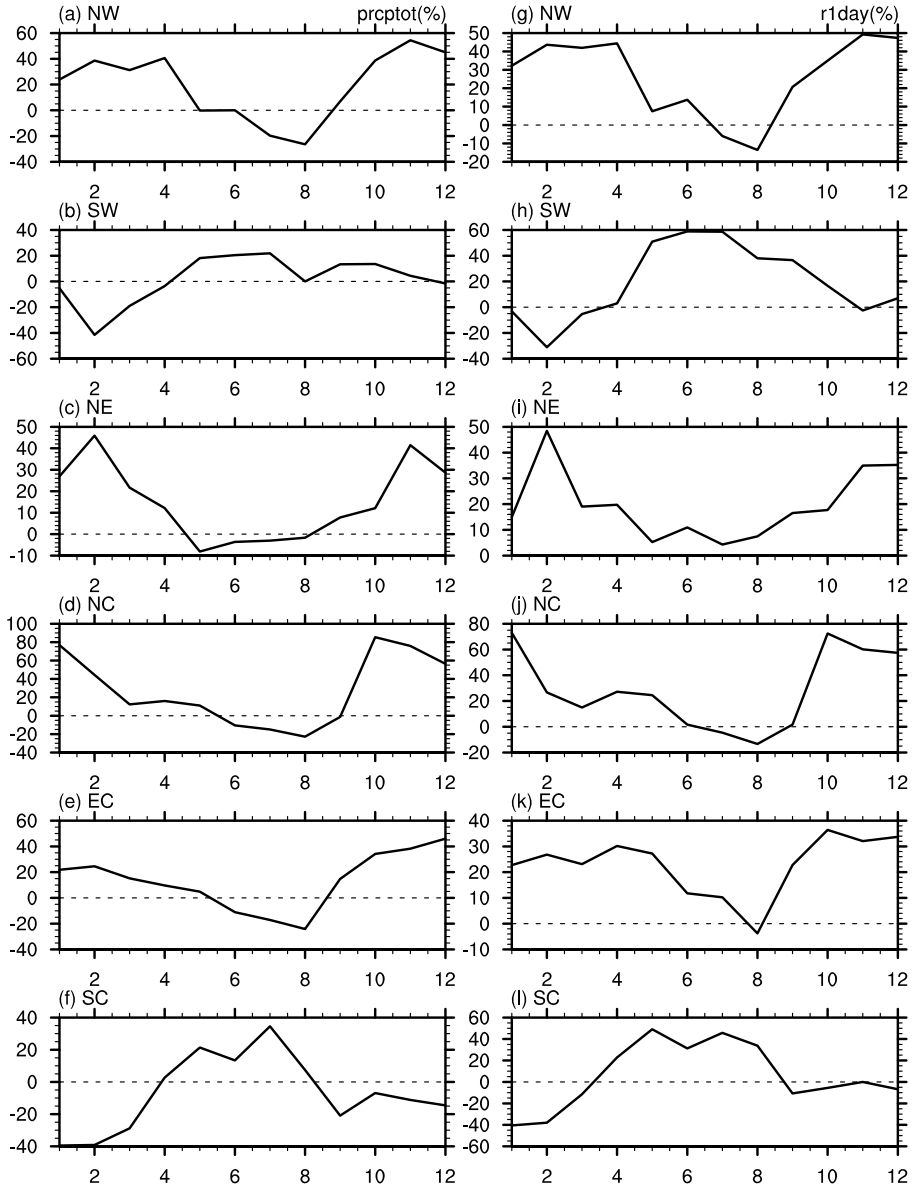

Fig. 8. (a–f) Percentage change (solid line) in monthly total precipitation amount (PRCPTOT, units: mm) averaged over six sub-regions: Northwest China, Southwest China, Northeast China, North China, East China, and South China (boxes shown in Fig. 1a). (g–l) The same as (a–f), but for the monthly maximum one-day precipitation (R1day, units: mm). The abscissa axis is months; the dashed line is the reference line.

Zhou, 2010). Interestingly, the change in CDD projected by coupled model results agrees with the results of the high-resolution model described in the present paper, i.e. a decrease in most parts of northern China and an increase in southern China (Jiang et al., 2009).

It is worth noting that some of the results derived from high-resolution regional climate models are also consistent with most of the projections for future precipitation change found in the current study. For example, the changes in annual mean precipitation over western China, with a decrease in the southern region and an increase in the northern region, agrees well with results derived from RegCM3, which employs a high resolution of 20 km (Gao et al., 2008). The changes in heavy rain days also concur well with results derived from RegCM2, the previous version of RegCM3 (Gao et al., 2002). The main difference is in northern China, where a potential drought projected by the RegCM3 model is not evident in the results from ECHAM5. In addition, precipitation changes over southeastern

China projected by ECHAM5 show much more variability in spatial signals than RegCM3. The response of precipitation in another regional climate model, PRECIS, under the IPCC B2 scenario shows a spatially consistent increase over all of China, except the southern Tibetan Plateau, the Sichuan Basin, and the southern part of northeastern China (Xu et al., 2006).

Although the high-resolution ECHAM5 model has shown an encouraging ability to simulate and project precipitation over China, some open questions remain. For example, the low-resolution CMIP3 models for IPCC AR4 generally underestimated precipitation over China, but the high-resolution ECHAM5 model clearly overestimated it. As to exactly what the preferable model resolution in climate change projection is remains an issue deserving of further study.

Acknowledgements. This work was jointly supported by the National Key Technologies R&D Program (Grant No. 2007BAC29B03), China-UK-Swiss Adapting to Climate Change in China Project (ACCC)-Climate Science, and the National Natural Science Foundation of China (Grant No. 40890054). The time-slice experiment was run on the Earth Simulator in Yokohama, Japan, as a collaboration between the Frontier Research Center for Global Change and the Max Planck Institute for Meteorology.

REFERENCES

Alexander, L., and Coauthors, 2006: Global observed changes in daily climate extremes of temperature and precipitation. *J. Geophys. Res.,* **111**, 1–22.

Allen, M., and W. Ingram, 2002: Constraints on future changes in climate and the hydrologic cycle. *Nature*, **419**, 224–232.

Bengtsson, L., M. Botzet, and M. Esch, 1996: Will greenhouse gas-induced warming over the next 50 years lead to higher frequency and greater intensity of hurricanes? *Tellus A,* **48**, 57–73.

Bengtsson, L., K. Hodges, M. Esch, N. Keenlyside, L. Kornblueh, J. Luo, and T. Yamagata, 2007: How may tropical cyclones change in a warmer climate? *Tellus A*, **59**(4), 539–561.

Bell, J., L. Sloan, and M. Snyder, 2004: Changes in extreme climatic events: A future climate scenario. *J. Climate,* **17**(1), 81–87.

Chen, H., T. Zhou, R. Neale, X. Wu, and G. Zhang, 2010: Performance of the new NCAR CAM3.5 model in East Asian Summer Monsoon simulations: Sensitivity to modifications of the convection scheme. *J. Climate*, **23**, 3657–3675.

Easterling, D., G. Meehl, C. Parmesan, S. Changnon, T. Karl, and L. Mearns, 2000: Climate extremes: observations, modeling, and impacts. *Science*, **289**, 2068–2074.

Gao, X., Z. Zhao, Y. Ding, R. Huang, and F. Giorgi, 2001: Climate change due to greenhouse effects in China as simulated by a regional climate model. *Adv. Atmos. Sci.*, **18**, 1224–1230.

Gao, X., Z. Zhao, and F. Giorgi, 2002: Changes of extreme events in regional climate simulations over East Asia. *Adv. Atmos. Sci.,* **19**(5), 927–941.

Gao, X., W. Lin, Z. Zhao, and F. Kucharsky, 2004: Simulation of climate and short-term climate prediction in China by CCM3 driven by observed SST. *Chinese J. Atmos. Sci.*, **28**, 63–76. (in Chinese)

Gao, X., Y. Xu, Z. Zhao, J. Pal, and F. Giorgi, 2006: On the role of resolution and topography in the simulation of East Asia precipitation. *Theoretical and Applied Climatology*, **86**, 173–185.

Gao, X., Y. Shi., R. Song, F. Giorgi, Y. Wang, and D. Zhang, 2008: Reduction of future monsoon precipitation over China: Comparison between a high resolution RCM simulation and the driving GCM. *Meteorology and Atmospheric Physics*, **100**, 73–86.

Giorgi, F., and M. Marinucci, 1996: An investigation of the sensitivity of simulated precipitation to the model resolution and its implications for climate studies. *Mon. Wea. Rev.*, **124**, 148–166.

IPCC, 2007a: Observations: Atmospheric surface and climate change. *Climate Change 2007: The Physical Science Basis. Contribution of Working Group I to the Fourth Assessment Report of the Intergovernmental Panel on Climate Change*, Solomon et al., Eds., Cambridge University Press, 240–316.

IPCC, 2007b: Climate models and their evaluation. *Climate Change 2007: The Physical Science Basis. Contribution of Working Group I to the Fourth Assessment Report of the Intergovernmental Panel on Climate Change*, Solomon et al., Eds., Cambridge University Press, 627–629.

IPCC, 2007c: Regional climate projection. *Climate Change 2007: The Physical Science Basis. Contribution of Working Group I to the Fourth Assessment Report of the Intergovernmental Panel on Climate Change*, Solomon et al., Eds., Cambridge University Press, 918–925.

Jungclaus, H., and Coauthors, 2006: Ocean circulation and tropical variability in the coupled model ECHAM5/MPI-OM. *J. Climate,* **19**, 3952–3972.

Jiang, Z., W. Chen, and J. Song, 2009: Projection and evaluation of the precipitation extremes indices over China based on seven IPCC AR4 coupled climate models. *Chinese J. Atmos. Sci.*, **33**(1), 1092120. (in Chinese)

Kusunoki, S., J. Yoshimura, H. Yoshimura, A. Noda, K. Oouchi, and R. Mizuta, 2006: Change of Baiu rain band in global warming projection by an atmospheric general circulation model with a 20-km grid size. *J. Meteor. Soc. Japan*, **84**(4), 581–611.

Karl, T., R. Knight, and N. Plummer, 1995: Trends in high-frequency climate variability in the twentieth century. *Nature,* **377**, 217–220.

Li, H., 2007: Observational analysis and numerical simulation of mid-summer precipitation and temperature

characteristic variations over China in the past 40 years. M. S. thesis, Institute of Atmospheric Physics, Chinese Academy of Sciences, 51–60. (in Chinese)

Li, H. M., L. Feng, and T. J. Zhou, 2010a: Multi-model Projection of July-August Climate Extreme Changes over China under CO_2 Doubling. Part I: Precipitation. *Adv. Atmos. Sci.*, doi: 10.1007/s00376-010-0013-4.

Li, H., A. Dai, T. Zhou, and J. Lu, 2010b: Responses of East Asian summer monsoon to historical SST and atmospheric forcing during 1950–2000. *Climate Dynamics*, **34**, 501–514, doi: 10.1007/s00382-008-0482-7.

Li, B., and T. Zhou, 2010: Projected climate changes over China under SERS A1B scenario: Multi-model ensemble and uncertainties. *Advances in climate changes*, **6**(4), 270–276.

Peterson, T., 2005: Climate change indices. *WMO Bulletin*, **54**(2), 83–86.

Qian, W., J. Fu, and Z. Yan, 2007: Decrease of light rain events in summer associated with a warming environment in China during 1961–2005, *Geophys. Res. Lett.,* **34**, L11705, doi: 10.1029/2007GL029631.

Tang, J., M. Zhao, and B. Su, 2006: Effects of model resolution on the simulation of regionally climatic extreme events. *Acta Meteorologica Sinica*, **64**(4), 432–442. (in Chinese)

Wehner, F., R. Smith, G. Bala, and P. Duffy, 2010: The effect of horizontal resolution on simulation of very extreme US precipitation events in a global atmosphere model. *Climate Dyn.*, **34**, 241–247, doi: 10.1007/s00382-009-0656-y.

Xie, P., M. Chen, S. Yang, A. Yatagai, T. Hayasaka, Y. Fukushima, and C. Liu 2007: A gauge-based analysis of daily precipitation over East Asia. *J. Hydrometeorology*, **8**(3), 607–626.

Xu, Y., and Coauthors, 2006: Climate change with PRECIS under B2 scenario over China. *Chinese Science Bulletin*, **51**(17), 2068–2074. (in Chinese)

You, Q., S. Kang, E. Aguilar, and Y. Yan, 2008: Changes in daily climate extremes in the eastern and central Tibetan Plateau during 1961–2005. *J. Geophys. Res.,* **113**, D07101, doi: 10.1029/2007JD009389.

Yu, R., W. Li, X. Zhang, Y. Liu, Y. Yu, H. Liu and T. Zhou, 2000: Climatic features related to eastern China summer rainfalls in the NCAR CCM3. *Adv. Atmos. Sci.,* **17**, 503–518.

Yu, R., and T. Zhou, 2007: Seasonality and three-dimensional structure of the interdecadal change in East Asian monsoon. *J. Climate*, **20**, 5344–5355.

Zhai, P., X. Zhang, H. Wan and X. Pan, 2005: Trends in total precipitation and frequency of daily precipitation extremes over China. *J. Climate*, **18**, 1096–1108.

Zhai, P., Z. Yan, and X. Zou, 2008: Climate extremes and climate-related disasters in China. *Regional Climate Studies of China*, Fu et al., Eds., Springer-Verlag Berlin Heidelberg, 313–339.

Zhang, L., and Y. Ding, 2008: Evaluation of extreme heavy precipitation in coupled ocean atmosphere general circulation models. *J. Appl. Meteor. Sci.*, **19**(6), 760–769.

Zhou, T., and Z. Li, 2002: Simulation of the East Asian summer monsoon by using a variable resolution atmospheric GCM. *Climate. Dyn.*, **19**, 167–180.

Zhou, T., and R. Yu, 2006: Twentieth century surface air temperature over China and the globe simulated by coupled climate models. *J. Climate*, **19**(22), 5843–5858.

Zhou, T., Y. Yu, H. Liu, W. Li, X. You, and G. Zhou, 2007: Progress in the development and application of climate ocean models and ocean-atmosphere coupled models in China. *Adv. Atmos. Sci.*, **24**(6), 729–738.

Zhou, T., L. Zhang, and H. Li, 2008a: Changes in global land monsoon area and total rainfall accumulation over the last half century. *Geophys. Res. Lett.*, **35**, L16707, doi: 10.1029/2008GL034881.

Zhou, T., R. Yu, H. Li, and B. Wang, 2008b: Ocean forcing to changes in global monsoon precipitation over the recent half century. *J. Climate*, **21**(15), 3833–3852.

Zhou, T., D. Gong, J. Li, and B. Li, 2009a: Detecting and understanding the multi-decadal variability of the East Asian summer monsoon—Recent progress and state of affairs. *Meteorologische Zeitschrift*, **18**(4), 455–467.

Zhou, T., B. Wu, and B. Wang, 2009b: How well do atmospheric general circulation models capture the leading modes of the interannual variability of Asian-Australian Monsoon? *J. Climate*, **22**, 1159–1173.